

Entropy production related properties of first passage process

Yunxin Zhang*

*Laboratory of Mathematics for Nonlinear Science,
Shanghai Key Laboratory for Contemporary Applied Mathematics,
Centre for Computational Systems Biology, School of Mathematical Sciences,
Fudan University, Shanghai 200433, China.*

(Dated: August 4, 2021)

Abstract

With nontrivial entropy production, first passage process is one of the most common nonequilibrium process in stochastic thermodynamics. Using one dimensional birth and death process as a model framework, approximated expressions of mean first passage time (FPT), mean total number of jumps (TNJ), and their coefficients of variation (CV), are obtained for the case far from equilibrium. Consequently, uncertainty relations for FPT and TNJ are presented. Generally, mean FPT decreases exponentially with entropy production, while mean TNJ decreases exponentially first and then tends to a starting site dependent limit. For forward biased process, the CV of TNJ decreases exponentially with entropy production, while that of FPT decreases exponentially first and then tends to a starting site dependent limit. For backward biased process, both CVs of FPT and TNJ tend to one for large absolute values of entropy production. Related properties about the case of equilibrium are also addressed briefly for comparison.

Keywords: First passage time, total number of jumps, entropy production, coefficient of variation, uncertainty relation

arXiv:2108.00121v2 [cond-mat.stat-mech] 3 Aug 2021

*Email: xyz@fudan.edu.cn

I. INTRODUCTION

Entropy production, which characterizes the degree of irreversibility (or dissipation), plays a key role in nonequilibrium stochastic thermodynamics [1–4]. In recent decades, many studies have been devoted to optimize the performance of stochastic thermodynamic machines, usually by reducing the total entropy production [5–16]. A general relation between nonequilibrium currents and entropy production, the thermodynamic uncertainty relation (TUR), is discovered and serves as a fundamental principle of nonequilibrium thermodynamics [17–30], which dictates that the precision of a nonequilibrium time-integrated current observable J is bounded from below by the inverse of the total entropy production (EP) σ , $(\langle J^2 \rangle - \langle J \rangle^2) / \langle J \rangle^2 \geq 2 / \langle \sigma \rangle$, with $\langle \cdot \rangle$ the average of random variables.

Recently, uncertainty relation between FPT and EP, sometimes called kinetic uncertainty relation (KUR), has attracted much attention. In [31], uncertainty relation for FPT is obtained by large deviation principle, which states that the precision of estimation of the FPT is limited by the total average dynamical activity. In [32], bounds on FPT fluctuation for currents are obtained by transferring bounds on the large-deviation function for currents, which show the FPT fluctuation is also bound by dissipation. In [33], a dissipation-time uncertainty relation is presented, which shows that the EP rate bounds the rate at which physical processes can be performed in stochastic systems far from equilibrium. In [34], the KUR on FPT is derived from the information inequality at stopping times, which shows that the precision of FPT is bounded from above by the mean TNJ. In [35], transition between long-lived states is discussed, and they found that there is a basic speed limit relating the typical excess heat dissipated throughout a transition and the rate amplification achievable. In [36], a TUR for FPT on continuous time Markov chains is derived, which shows that the coefficient of variation of the FPT is bounded from below by an expression that combines the entropy production from the transitions between internal states and the fluxes to absorbing boundaries.

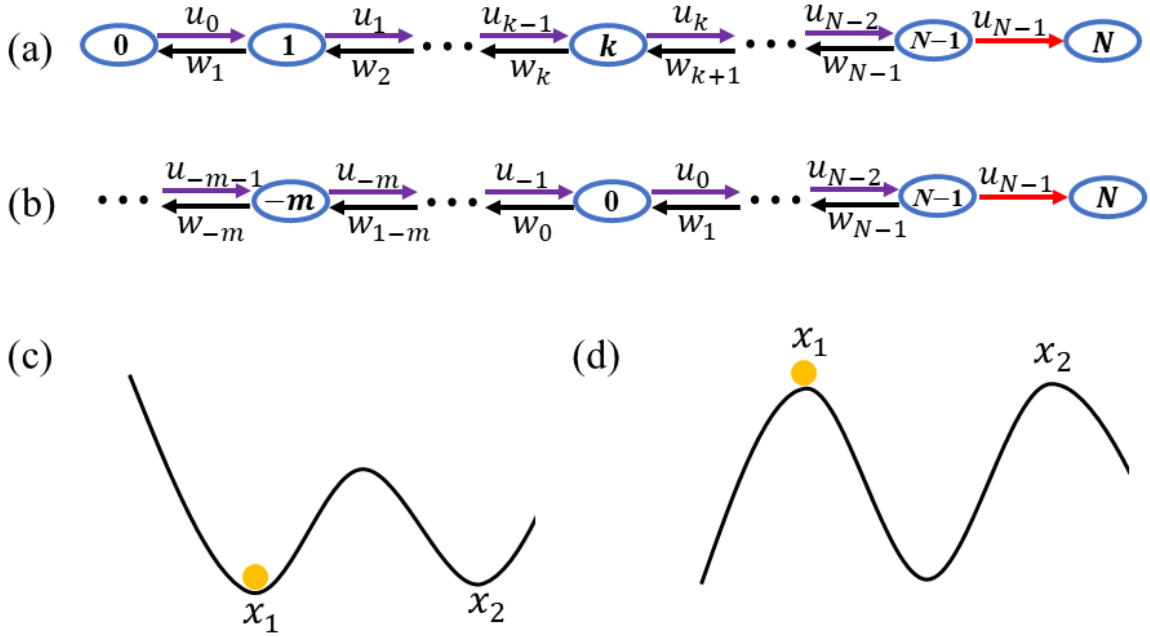


FIG. 1: First passage process discussed in this study, with site N an absorbing boundary. (a) Finite state cases with site 0 a reflecting boundary. (b) Infinite state cases with $-\infty$ a reflecting boundary. (c,d) Two typical examples of first passage process, with the random particle starting from position x_1 to reach absorbing boundary x_2 .

In general, EP (or heat dissipation) is essential to first passage process. To find out EP related properties, this study considers a simple one-dimensional birth and death process (continuous-time Markov chain as depicted in Fig. 1(a)), where the forward jump rate from site k to $k + 1$ is denoted by u_k , and the backward jump rate from site k to $k - 1$ is denoted by w_k . The boundary site N is assumed to be an

absorbing boundary, while the boundary site 0 is assumed to be a reflecting boundary. Results are similar if boundary site 0 is also an absorbing boundary, or if there are infinite sites as depicted in Fig. 1(b). This model process can be used sometimes to discuss the transition in a system with two stable steady states as shown in Fig. 1(c,d) [37, 38].

II. FIRST PASSAGE PROCESS WITH FINITE STATES

The probability density $p_k(s, t)$ that a random particle initiated at site k to reach the absorbing boundary N at time t and with EP s satisfies the following backward master equation

$$\partial_t p_k(s, t) = u_k p_{k+1}(s - \ln(u_k/w_{k+1}), t) + w_k p_{k-1}(s - \ln(w_k/u_{k-1}), t) - (u_k + w_k) p_k(s, t), \quad (1)$$

with $\ln(u_k/w_{k+1})$ and $\ln(w_k/u_{k-1})$ entropy productions ($k_B = 1$) during one forward and backward jump, respectively [2, 39, 40]. From Eq. (1), the mean EP $S_k := \int_{-\infty}^{\infty} s \int_0^{\infty} p_k(s, t) dt ds$ during the passage process from site k to boundary N satisfies

$$u_k S_{k+1} + w_k S_{k-1} - (u_k + w_k) S_k = - \left(u_k \ln \frac{u_k}{w_{k+1}} + w_k \ln \frac{w_k}{u_{k-1}} \right). \quad (2)$$

The mean FPT $T_k := \int_0^{\infty} t \int_{-\infty}^{\infty} p_k(s, t) ds dt$, and the second moment $T_k^{(2)} := \int_0^{\infty} t^2 \int_{-\infty}^{\infty} p_k(s, t) ds dt$, satisfy

$$u_k T_{k+1} + w_k T_{k-1} - (u_k + w_k) T_k = -1, \quad (3)$$

$$u_k T_{k+1}^{(2)} + w_k T_{k-1}^{(2)} - (u_k + w_k) T_k^{(2)} = -2T_k. \quad (4)$$

The probability $q_k(n)$ that a random particle initiated at site k to reach the absorbing boundary N with TNJ n satisfies the following backward master equation

$$u_k q_{k+1}(n-1) + w_k q_{k-1}(n-1) - (u_k + w_k) q_k(n) = 0. \quad (5)$$

So, the mean TNJ $n_k := \sum_{n=0}^{\infty} n q_k(n)$, and the second moment $n_k^{(2)} := \sum_{n=0}^{\infty} n^2 q_k(n)$, satisfy

$$u_k n_{k+1} + w_k n_{k-1} - (u_k + w_k) n_k = -(u_k + w_k), \quad (6)$$

$$u_k n_{k+1}^{(2)} + w_k n_{k-1}^{(2)} - (u_k + w_k) n_k^{(2)} = -(2n_k - 1)(u_k + w_k). \quad (7)$$

By usual algebraic calculations, explicit expressions of mean EP S_k , mean FPT T_k , mean TNJ n_k , as well as the second moments $T_k^{(2)}$ and $n_k^{(2)}$ can be obtained by solving Eqs. (2,3,4,6,7), see **Supplemental Materials**. To illustrate the influence of EP S_k on FPT and TNJ, we consider the particular case with $u_k \equiv u$ and $w_k \equiv w = ru$. It can be shown that,

$$S_k(r) = -(N - k - 1) \ln r, \quad (8)$$

$$T_k(r) = \frac{N - k}{u(1 - r)} + \frac{r^{N+1} - r^{k+1}}{u(1 - r)^2}, \quad (9)$$

$$n_k(r) = \frac{(1 + r)(N - k)}{1 - r} + \frac{(1 + r)(r^{N+1} - r^{k+1})}{(1 - r)^2}, \quad (10)$$

and

$$T_k^{(2)}(r) - T_k^2(r) = \frac{(N - k)(1 + r)}{u^2(1 - r)^3} + \frac{r^{2N+2} - r^{2k+2}}{u^2(1 - r)^4} + o(r), \quad (11)$$

$$n_k^{(2)}(r) - n_k^2(r) = \frac{4(N - k)r(1 + r)}{(1 - r)^3} + \frac{(1 + r)^2(r^{2N+2} - r^{2k+2})}{(1 - r)^4} + o(r), \quad (12)$$

with $o(r)$ the high (low) order term for $r \rightarrow 0$ ($r \rightarrow \infty$).

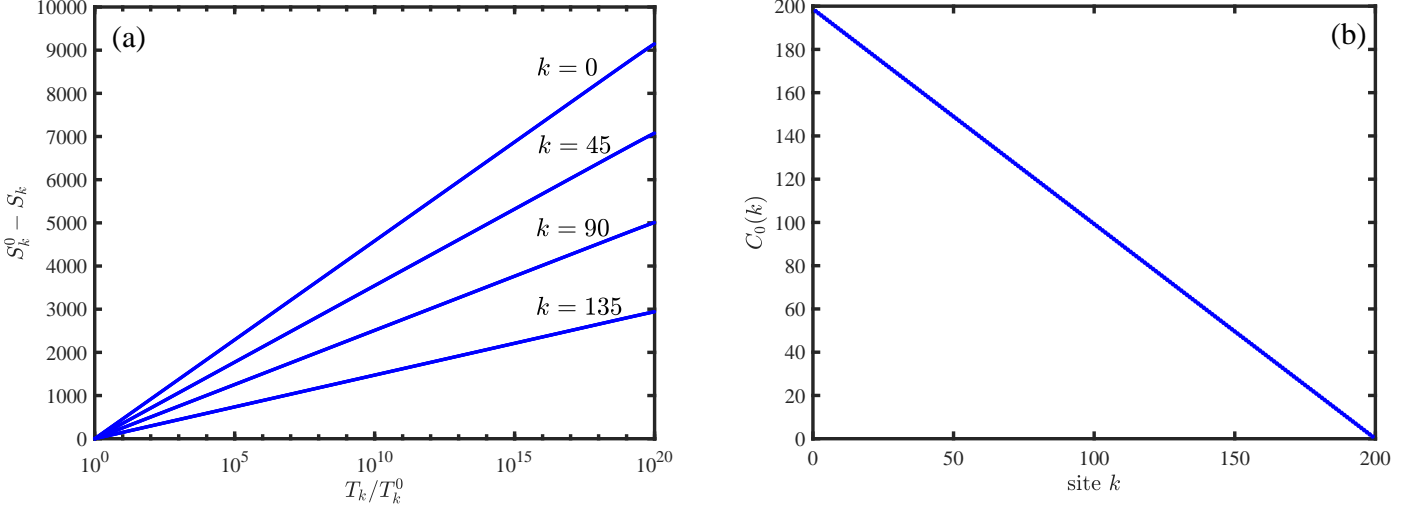


FIG. 2: Relationship between EP and the ratio of mean FPT for the process depicted in Fig. 1(a), with $N = 200$ therein. For each starting site k , 1000 values of S_k and T_k are calculated, see Eqs. (S8,S9). In the first calculation, all forward rates $\{u_k^{(1)}\}$ and backward rates $\{w_k^{(1)}\}$ are randomly selected in interval $(0.5, 3)$. Then in following calculations, backward rates $\{w_k\}$ remain unchanged while forward rates change according to $u_k^{(l+1)} = \gamma u_k^{(l)}$ with $\gamma = 1.05$. For convenience, T_k^0 is chosen to be the minimal value of T_k , and S_k^0 is the EP according to T_k^0 . (a) $S_k^0 - S_k$ versus T_k/T_k^0 , with starting site $k = 0, 45, 90, 135$ respectively. Results show that $T_k/T_k^0 \approx C_1(k) \exp(-(S_k - S_k^0)/C_0(k))$. (b) $C_0(k)$ obtained by fitting to $T_k/T_k^0 = C_1(k) \exp(-(S_k - S_k^0)/C_0(k))$, see Eq. (13). For this example $C_0(k) \approx N - k - 1$ while $C_1(k) \approx 0.9$ is almost constant.

A. Forward biased process with $r = w/u < 1$

If the backward rate w is fixed while forward rate u is large enough, *i.e.*, $r \ll 1$, then Eq. (9) implies $T_k \sim (N - k)r/w$, and

$$\frac{T_k(r_1)}{T_k(r_0)} \sim \frac{r_1}{r_0} = \exp\left(-\frac{S_k(r_1) - S_k(r_0)}{N - k - 1}\right) =: \exp\left(-\frac{\Delta S_k}{N - k - 1}\right). \quad (13)$$

Numerical calculations show this relationship between $T_k(r_1)/T_k(r_0)$ and ΔS_k is still true for general nonconstant rates $\{u_k\}$ and $\{w_k\}$ which satisfy $w_k/u_k \equiv r \ll 1$, see Fig. 2.

From Eqs. (9,10,11,12), for $r \ll 1$,

$$T_k(r) \lesssim \frac{(N - k)r}{w(1 - r)}, \quad (14)$$

$$n_k(r) \lesssim \frac{(1 + r)(N - k)}{(1 - r)}, \quad (15)$$

$$T_k^{(2)}(r) - T_k^2(r) \sim \frac{(N - k)(1 + r)r^2}{w^2(1 - r)^3}, \quad (16)$$

$$n_k^{(2)}(r) - n_k^2(r) \sim \frac{4(N - k)r(1 + r)}{(1 - r)^3}. \quad (17)$$

Therefore,

$$\text{CV}[T_k(r)] := \frac{T_k^{(2)}(r) - T_k^2(r)}{T_k^2(r)} \gtrsim \frac{1 + r}{(N - k)(1 - r)} = \frac{1 + \exp(-S_k(r)/(N - k - 1))}{(N - k)[1 - \exp(-S_k(r)/(N - k - 1))]} \rightarrow \frac{1}{N - k} \quad (18)$$

which means that CV of FPT decreases with EP S_k , and tends to its lower limit $\text{CV}[T_k(0)] = 1/(N - k)$

with $S_k \rightarrow \infty$, see Fig 3. Eq. (18) can be rewritten as follows,

$$\frac{T_k^2(r)}{T_k^{(2)}(r) - T_k^2(r)} \lesssim \frac{(N-k)(1-r)}{1+r} \leq n_k(r), \quad (19)$$

which is the KUR obtained in [34]. From Eq. (18) and Fig 3, $\text{CV}[T_k(r)] - \text{CV}[T_k(0)] \gtrsim 2r/(N-k)$, so CV of FPT decreases exponentially to its limit $\text{CV}[T_k(0)]$ when $S_k \rightarrow \infty$.

For TNJ, we obtain from Eqs. (15,17) that

$$\begin{aligned} \text{CV}[n_k(r)] &:= \frac{n_k^{(2)}(r) - n_k^2(r)}{n_k^2(r)} \gtrsim \frac{4r}{(N-k)(1-r^2)} \\ &= \frac{4 \exp(-S_k(r)/(N-k-1))}{(N-k)[1 - \exp(-2S_k(r)/(N-k-1))]} \sim \frac{4 \exp(-S_k(r)/(N-k-1))}{(N-k)}, \end{aligned} \quad (20)$$

which decreases to 0 exponentially with entropy S_k , see Fig 3.

Eqs. (14,15) and Fig 3 show that, with $S_k \rightarrow \infty$, T_k decreases to 0 and n_k decreases to its lower limit $N-k$, both exponentially.

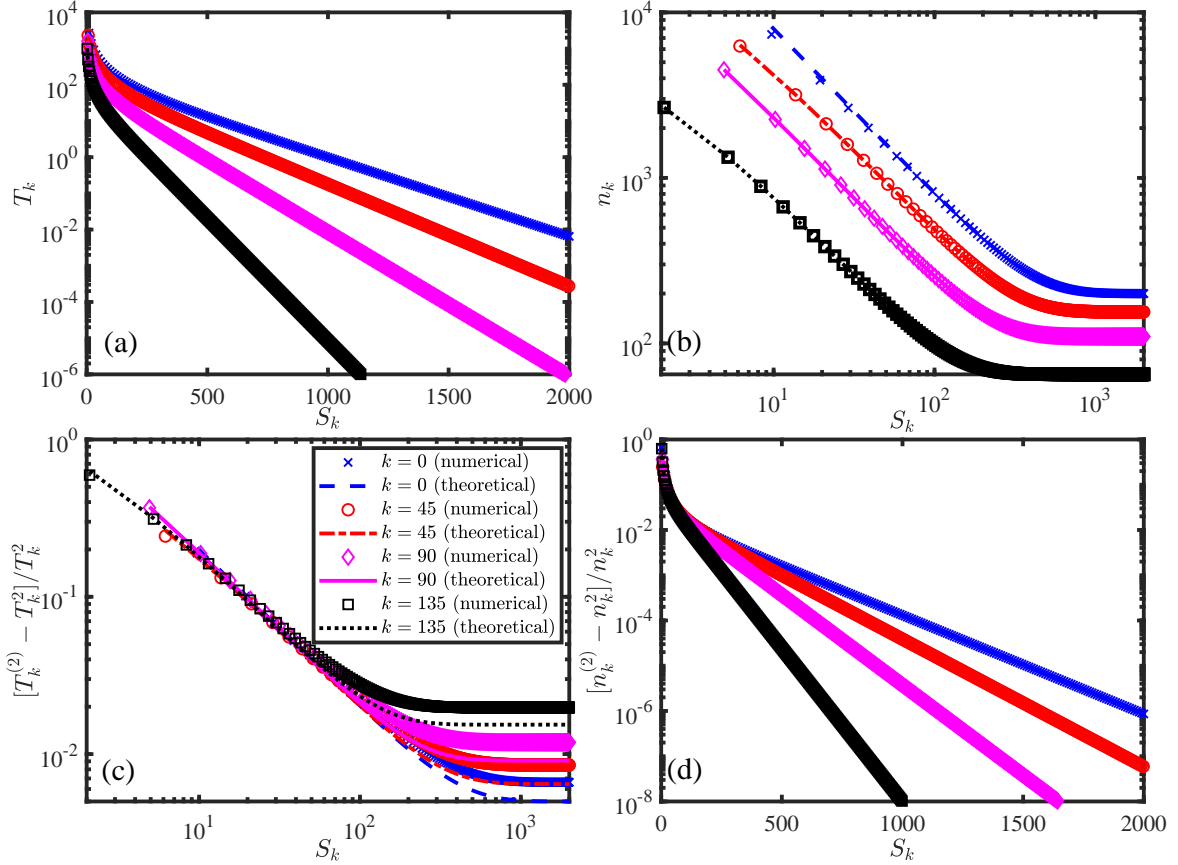


FIG. 3: Mean FPT T_k , mean TNJ n_k , and $[T_k^{(2)} - T_k^2]/T_k^2$, $[n_k^{(2)} - n_k^2]/n_k^2$, with the change of EP S_k , and for starting site $k = 0, 45, 90, 135$ respectively. Points are obtained numerically by formulations given in Eqs. (S8,S9,S10,S11,S12), and with parameter values randomly selected in the same intervals as in Fig. 2. Lines are obtained from the bounds given in Eqs. (14,15,18,20), with r replaced by $\exp(-S_k/(N-k-1))$, and w in Eq. (14) replaced by the harmonic mean of $\{w_i\}_{i=k}^{N-1}$.

On the other hand, if forward rate u is fixed while backward rate $w \rightarrow 0$, then Eq. (9) gives $T_k(r) \lesssim (N-k)/[u(1-r)]$, and results in Eq. (15,18,19,20) still hold true, see Fig. S1. Since $T_k(r) - T_k(0) \sim (N-k)r/u$, $T_k(r)$ decreases exponentially to its limit $(N-k)/u$ with $S_k \rightarrow \infty$.

Results given in Eqs. (14,15,18,20) are also true for nonconstant rates $\{u_k\}$ and $\{w_k\}$ which satisfy $w_k/u_k \equiv r \ll 1$ (or $S_k \gg 0$ equivalently), see Fig 3. Generally, if both forward rates $\{u_k\}$ and backward

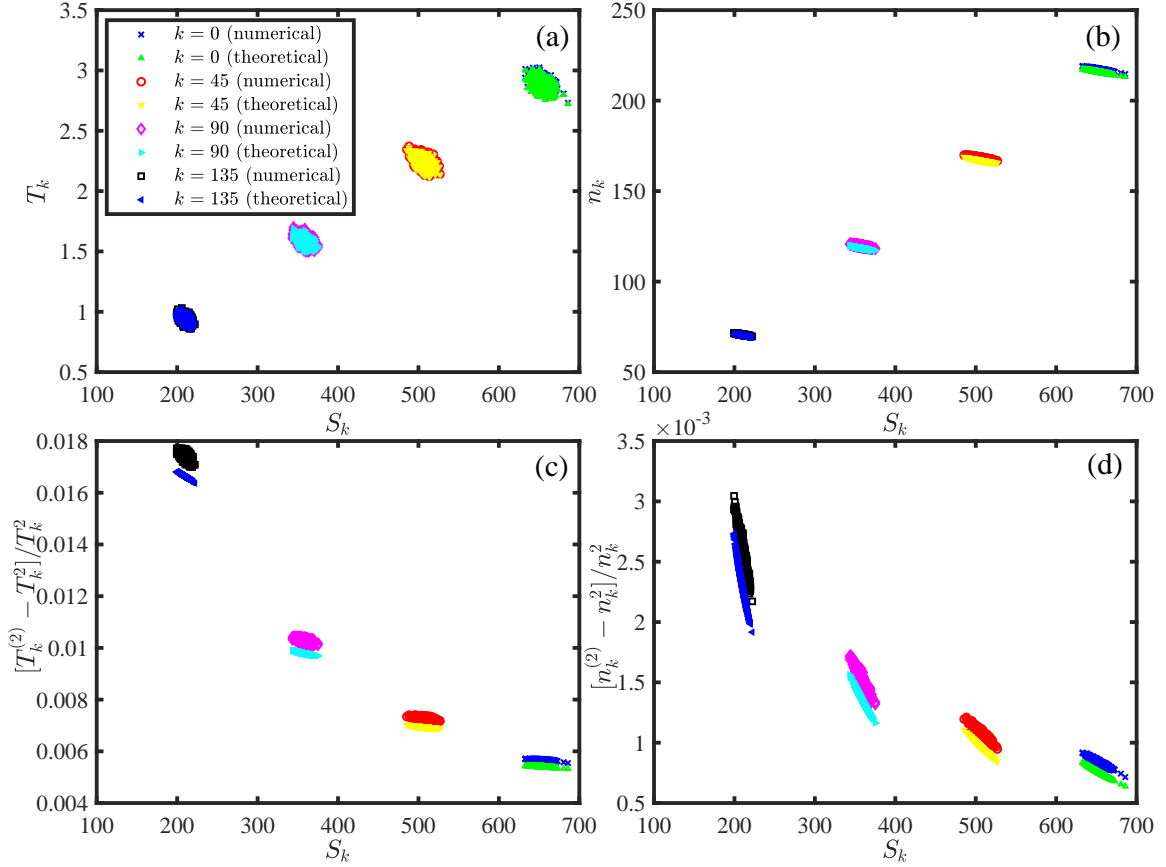


FIG. 4: Results for randomly selected values of both forward rates $\{u_i\}$ and backward rates $\{w_i\}$. We do 1000 calculations, and in each calculation, $N = 200$ is fixed, while $\{w_i\}$ are randomly selected in interval $(1, 5)$, and $\{u_i\}$ are randomly selected in interval $(50, 100)$. The theoretical points (marked by varies triangles) are obtained according to the bounds given in Eqs. (14,15,18,20), with r replaced by $\exp(-S_k/(N - k - 1))$, and w in Eq. (14) replaced by the harmonic mean of $\{w_i\}_{i=k}^{N-1}$. Numerical values are obtained as in Fig. 3.

rates $\{w_k\}$ are chosen randomly but keeping EP S_k positive, inequalities given in Eqs. (18,20) are also true, but the ones given in Eqs. (14,15) may not, see Fig 4. However, for large S_k , mean FPT T_k and mean TNJ n_k can be well approximated by the upper bounds given in Eqs. (14,15). Note that, for randomly selected rates $\{u_k\}$ and $\{w_k\}$, the ratio r in Eqs. (14,15,18,20) should be replaced by $\exp(-S_k/(N - k - 1))$, and w (or u) in Eq. (14) should be replaced by the harmonic mean of $\{w_i\}_{i=k}^{N-1}$ (or $\{u_i\}_{i=k}^{N-1}$).

B. Backward biased process with $r = w/u > 1$

If backward rate w is fixed while forward rate u is small enough ($r \gg 1$), then Eqs. (9) implies $T_k(r) \sim r^N/w$. So,

$$\frac{T_k(r_1)}{T_k(r_0)} \sim \left(\frac{r_1}{r_0}\right)^N = \exp\left(-\frac{N\Delta S_k}{N - k - 1}\right). \quad (21)$$

Again this approximation is still true for nonconstant rates $\{u_k\}$ and $\{w_k\}$ which satisfy $w_k/u_k \equiv r \gg 1$, see Fig. S2.

According to Eqs. (9,10,11,12), for $r \gg 1$,

$$T_k(r) \lesssim \frac{r^{N+2} - r^{k+2}}{w(1-r)^2}, \quad n_k(r) \lesssim \frac{(1+r)(r^{N+1} - r^{k+1})}{(1-r)^2}, \quad (22)$$

$$T_k^{(2)}(r) - T_k^2(r) \sim \frac{r^{2N+4} - r^{2k+4}}{w^2(1-r)^4}. \quad (23)$$

$$n_k^{(2)}(r) - n_k^2(r) \sim \frac{(1+r)^2(r^{2N+2} - r^{2k+2})}{(1-r)^4}. \quad (24)$$

Therefore,

$$\text{CV}[T_k(r)] \sim \text{CV}[n_k(r)] \gtrsim \frac{r^{N-k} + 1}{r^{N-k} - 1} = \frac{\exp(-(N-k)S_k(r)/(N-k-1)) + 1}{\exp(-(N-k)S_k(r)/(N-k-1)) - 1} \rightarrow 1. \quad (25)$$

Similar as in the *forward biased* cases, results given in Eqs. (22,25) are still valid for nonconstant rates $\{u_k\}$ and $\{w_k\}$ which satisfy $w_k/u_k \equiv r \gg 1$, see Fig. S3. Generally, if both $\{u_k\}$ and $\{w_k\}$ are selected randomly but keeping EP S_k negative, then for the absolute value of S_k large enough, *i.e.*, for process far from equilibrium, $\text{CV}[T_k]$ and $\text{CV}[n_k]$ are almost one, and T_k, n_k can be well approximated by the bounds given in Eq. (22), see Fig. S4. It can be easily shown that the KUR given in Eq. (19) is also valid.

Meanwhile, if forward rate u is fixed while backward rate $w = ru$ tends to infinity, then Eq. (9) implies $T_k(r) \sim r^{N-1}/u$, which means

$$\frac{T_k(r_1)}{T_k(r_0)} \sim \left(\frac{r_1}{r_0}\right)^{N-1} = \exp\left(-\frac{(N-1)\Delta S_k}{N-k-1}\right). \quad (26)$$

At the same time, $T_k(r) \lesssim (r^{N+1} - r^{k+1})/[u(1-r)^2]$, and results for $n_k(r)$ and $\text{CV}[T_k(r)], \text{CV}[n_k(r)]$ given in Eqs. (22,25) still hold, see Fig. S5.

In summary, $T_k(r_1)/T_k(r_0) \sim C_1(k) \exp(-\Delta S_k/C_0(k))$ if backward rate $\{w_k\}$ are fixed while forward rate $\{u_k\}$ tend to infinity or zero, or forward rate $\{u_k\}$ are fixed while backward rate $\{w_k\}$ tend to infinity, see Eqs. (13,21,26) and Figs. 2,S2,S5. The ratio r of backward rate to forward rate tends to 0 or infinity means the process is far from equilibrium. So the results obtained here are consistent with the ones obtained previously [35]. For fixed $\{u_k\}$, if backward rates $\{w_k\}$ tend to zero, then the process becomes a deterministic motion. So $T_k \rightarrow 1/u_k + \dots + 1/u_{N-1} = (N-k)/u$ and $n_k \rightarrow N-k$, see Eqs. (9,10) and Fig. S1. For either $\{u_k\}$ tend to infinity or $\{w_k\}$ tend to 0, mean TNJ n_k decreases to its lower bound $N-k$, $\text{CV}[T_k]$ decreases to its lower bound $1/(N-k)$, and $\text{CV}[n_k]$ decreases to 0 exponentially with EP S_k , see Eqs. (10,18,20) and Figs. 3 and S1. On the contrary, for either $\{u_k\}$ tend to 0 or $\{w_k\}$ tend to infinity, both mean FPT T_k and mean TNJ n_k increase to infinity, while $\text{CV}[T_k]$ and $\text{CV}[n_k]$ are around 1, see Eqs. (9,10,22,25) and Figs. S3 and S5.

For $r \ll 1$, uncertainty relations given in Eqs. (18,19,20) are established, while for $r \gg 1$, we have the one as given in Eq. (25). Numerical calculations show that, for randomly selected rates $\{u_k\}$ and $\{w_k\}$, the bounds given in Eqs. (14,15,18,20) are good approximations of $T_k, n_k, \text{CV}[T_k], \text{CV}[n_k]$ if EP S_k are positive and large enough, see Fig. 4. Meanwhile, if EP S_k is negative and its absolute value is large enough, the bounds given in Eqs. (22,25) are also good approximations of $T_k, n_k, \text{CV}[T_k], \text{CV}[n_k]$, see Fig. S4.

C. Cases of equilibrium with $r = 1$

It can be shown directly from Eqs. (S9,S11), or by taking the limit $r \rightarrow 1$ in Eqs. (9,10), that

$$T_k = (N-k)(N+k+1)/2u, \quad (27)$$

$$n_k = (N-k)(N+k+1), \quad (28)$$

Both of them decrease with starting site k . Meanwhile, it can be obtained that, for $r = 1$,

$$\text{CV}[T_k] = \frac{(2N+1)^2 + 1}{3(N-k)(N+k+1)} - \frac{2}{3}, \quad (29)$$

$$\text{CV}[n_k] = \frac{2N(N+1) + 2k(k+1) - 1}{3(N-k)(N+k+1)} = \text{CV}[T_k] - \frac{1}{(N-k)(N+k+1)}, \quad (30)$$

both increase with starting site k . Numerical calculations show that Eqs. (27,28,29,30) are valid for general equilibrium cases, in which $w_k = u_k$ but may be different at different site k , see Fig. S6. Note that, for general equilibrium cases, u in Eq. (27) should be replaced by the harmonic mean of $\{u_i\}_{i=k}^{N-1}$.

III. FIRST PASSAGE PROCESS WITH INFINITE STATES

For the first passage process depicted in Fig. 1(b), with $-\infty$ a reflecting boundary, we obtain from Eqs. (3,4,6,7) that, for $u_k \equiv u$, $w_k \equiv w$ and $r = w/u$,

$$T_k = \frac{N-k}{u-w}, \quad n_k = \frac{(u+w)(N-k)}{u-w} = (u+w)T_k, \quad (31)$$

$$\text{CV}[T_k] = \frac{u+w}{(N-k)(u-w)} = \frac{1 + \exp(-S_k/(N-k-1))}{(N-k)[1 - \exp(-S_k/(N-k-1))]}, \quad (32)$$

$$\text{CV}[n_k] = \frac{4uw}{(N-k)(u^2 - w^2)} = \frac{4 \exp(-S_k/(N-k-1))}{(N-k)[1 - \exp(-2S_k/(N-k-1))]}, \quad (33)$$

where we assume $0 \leq r < 1$, *i.e.*, $u > w$, otherwise $T_k = n_k = \infty$.

For fixed w and r , $r_0 \ll 1$, $T_k(r)/T_k(r_0) \sim r/r_0 = \exp(-\Delta S_k/(N-K-1))$, which is the same as listed in Eq. (13). Meanwhile, $T_k^2/[T_k^{(2)} - T_k^2] = 1/\text{CV}[T_k] = n_k[(1-r)/(1+r)]^2 \leq n_k$, so the KUR is established, see Eq. (19) and [34]. From Eqs. (32,33), one can easily show $\text{CV}[n_k]/\text{CV}[T_k] = 4uw/(u+w)^2 < 1$, so the uncertainty of TNJ is always less than that of the FPT. Numerical calculations show that this is also true for the finite state cases provided $r < 1$, see Fig. 3,S1,S7. Note that, the lower bounds listed in Eqs. (18,20) of $\text{CV}[T_k]$ and $\text{CV}[n_k]$ for finite state cases are the same as the ones given in Eq. (32,33) for infinite state cases. Meanwhile, Eq. (30) and Fig. S6 indicate that $\text{CV}[n_k] < \text{CV}[T_k]$ is also true for general equilibrium cases.

The processive motion of motor proteins (such as kinesin and dynein) along microtubule in cells can be well described by the one dimensional birth and death process depicted in Fig. 1(b) [41–43]. Experiments show that the forward stepping of motor proteins is tightly coupled with ATP hydrolysis, *i.e.*, one ATP molecule is consumed in each forward step (about 8.2 nm), while the backward sliding is ATP free [44, 45]. To analyze the energy efficiency of motor proteins, we need to know how many ATP molecules are consumed during the motion from starting site k to reach boundary N first.

Let n_k^+ (n_k^-) be the mean total numbers of forward (backward) jumps during the process. Obviously, $n_k^+ + n_k^- = n_k$ and $n_k^+ - n_k^- = N - k$. So, according to Eq. (31), we have $n_k^+ = (N - k)/(1 - r)$ and $n_k^- = r(N - k)/(1 - r)$. For a given sample path of the first passage process with total number of forward jumps \tilde{n}_k^+ and total number of backward jumps \tilde{n}_k^- , the energy efficiency of ATP molecule is

$$\tilde{\eta}_k^{\text{ATP}} = \frac{\tilde{n}_k^+ - \tilde{n}_k^-}{\tilde{n}_k^+} = \frac{N - k}{\tilde{n}_k^+}.$$

So $\langle 1/\tilde{\eta}_k^{\text{ATP}} \rangle = \langle \tilde{n}_k^+ \rangle / (N - k) = n_k^+ / (N - k) = 1/(1 - r)$. By Jensen's inequality, the mean value of energy efficiency $\eta_k^{\text{ATP}} = \langle \tilde{\eta}_k^{\text{ATP}} \rangle$ satisfies

$$\eta_k^{\text{ATP}} \geq 1 - r, \quad (34)$$

which decreases (increases) with ratio $r = w/u$ (EP S_k).

Moreover, it can be shown that CVs of total forward and backward jumps are as follows,

$$\text{CV}[n_k^+] = \frac{r(1+r)}{(1-r)(N-k)}, \quad \text{CV}[n_k^-] = \frac{1+r}{(1-r)r(N-k)}. \quad (35)$$

One can show that $\text{CV}[n_k^+] = r^2 \text{CV}[n_k^-]$, and $\text{CV}[n_k^+] = (1+r)^2 \text{CV}[n_k]/4 < \text{CV}[n_k] = 4r^2 \text{CV}[n_k^-]/(1+r)^2 < \text{CV}[n_k^-]$. Evidently, $\text{CV}[n_k^+]$ increases (decreases) with ratio r (EP S_k), while $\text{CV}[n_k^-]$ attains its minimum $(\sqrt{2}+1)^2/(N-k)$ when $r = \sqrt{2}-1$, at which $\eta_k^{\text{ATP}} \geq 2 - \sqrt{2}$, $n_k^- = (N-k)/\sqrt{2}$, $n_k = (\sqrt{2}+1)(N-k)$ and $\text{CV}[n_k^+] = 1/(N-k)$, $\text{CV}[n_k] = 2/(N-k)$, $\text{CV}[T_k] = (\sqrt{2}+1)/(N-k)$. Although, both n_k^+ and n_k^- decrease with starting site k , $\text{CV}[n_k^+]$ and $\text{CV}[n_k^-]$ increase with k .

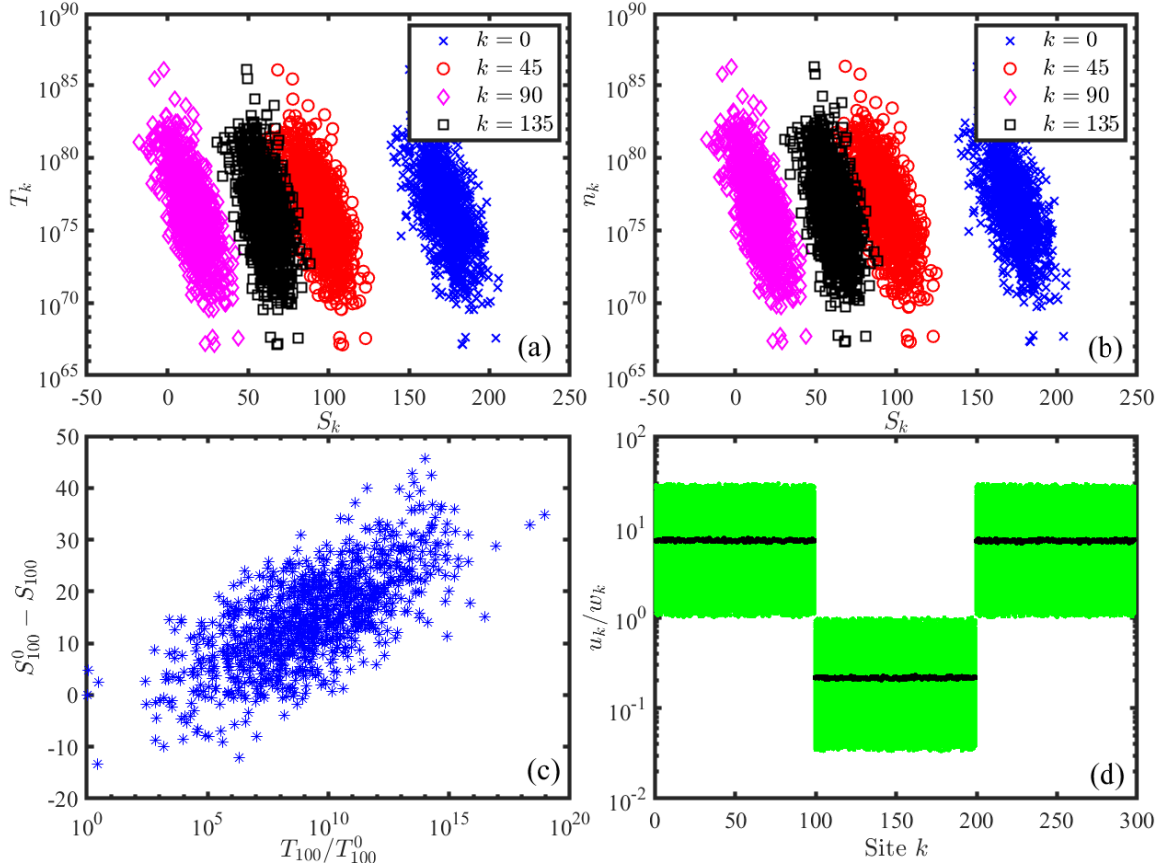


FIG. 5: Results for the first passage process as depicted in Fig. 1(c) (with x_2 therein assumed to be the absorbing boundary N as in Fig. 1(a)). For $k < 100$ and $k \geq 200$, $\{u_k\}$ and $\{w_k\}$ are randomly selected in intervals $(0.5, 3)$ and $(0.1, 0.5)$ respectively, while for $100 \leq k < 200$ their selection intervals are exchanged with each other. $N = 300$ is used, and altogether 1000 groups of $\{u_k\}$ and $\{w_k\}$ are used. In (d), ratio u_k/w_k is plotted as small light dot, and their mean value is plotted as large thick dots. Values of S_k , T_k and n_k are obtained by formulations given in Eqs. (S8,S9,S11) respectively.

Finally, we address briefly the usual transition between two steady states, as depicted in Fig. 1(c). With x_2 assumed to be the absorbing boundary N , the plots in Fig. 5 show that, from any starting site k , both mean FPT T_k and mean TNJ n_k decrease with EP S_k , and roughly in an exponential manner. For the transition depicted in Fig. 1(d), results are similar, see Fig. S8.

IV. CONCLUSIONS

In conclusion, the entropy production S related properties of first passage process are discussed extensively in this study. For process with either finite or infinite internal states, approximated expressions of mean FPT T , mean TNJ n , and their coefficients of variation, $\text{CV}[T]$ and $\text{CV}[n]$, are obtained for

either $S \gg 0$ or $S \ll 0$. Generally, $CV[n] < CV[T]$ for forward biased (or equilibrium) process, while for backward biased process, both of them tend to 1 quickly with the increase of the absolute value of entropy production S . Roughly speaking, mean FPT decreases exponentially with entropy production S . For the mean TNJ, it decreases exponentially first, and then tends to a starting site dependent limit finally. For equilibrium cases with $S = 0$, approximated expressions of mean FPT T , mean TNJ n and $CV[T]$, $CV[n]$ are also obtained, which mainly depend on the starting site and the position of absorbing boundary. Although most of expressions are obtained simply under the homogeneous assumption, in which values of forward rates and backward rates are independent of state, numerical calculations show they are also reasonable for general biased process, with forward rates always greater (or always less) than backward rates.

-
- [1] K. Sekimoto, *Stochastic Energetics* (Springer Berlin Heidelberg, 2010).
 - [2] U. Seifert, Rep. Prog. Phys. **75**, 126001 (2012).
 - [3] N. Shiraishi and K. Saito, J. Stat. Phys. **174**, 433 (2019).
 - [4] U. Seifert, Annu. Rev. Condens. Ma. P. **10**, 171 (2019).
 - [5] T. Schmiedl and U. Seifert, Phys. Rev. Lett. **98**, 108301 (2007).
 - [6] A. Gomez-Marin, T. Schmiedl, and U. Seifert, J. Chem. Phys. **129**, 024114 (2008).
 - [7] E. Aurell, C. Mejía-Monasterio, and P. Muratore-Ginanneschi, Phys. Rev. Lett. **106**, 250601 (2011).
 - [8] N. Golubeva and A. Imparato, Phys. Rev. Lett. **109**, 190602 (2012).
 - [9] P. Muratore-Ginanneschi, C. Mejía-Monasterio, and L. Peliti, J. Stat. Phys. **150**, 181 (2013).
 - [10] J. M. Horowitz and A. P. Solon, Phys. Rev. Lett. **120**, 180605 (2018).
 - [11] Y. Zhang, EPL **128** (2019).
 - [12] Y. Zhang, J. Stat. Phys. **178**, 1336 (2020).
 - [13] P. Abiuso and M. Perarnau-Llobet, Phys. Rev. Lett. **124**, 110606 (2020).
 - [14] T. K. Saha, J. N. E. Lucero, J. Ehrich, D. A. Sivak, and J. Bechhoefer, Proc. Natl. Acad. Sci. USA **118**, e2023356118 (2021).
 - [15] B. Remlein and U. Seifert, Phys. Rev. E **103**, L050105 (2021).
 - [16] G. Gronchi and A. Puglisi, Phys. Rev. E **103**, 052134 (2021).
 - [17] A. C. Barato and U. Seifert, Phys. Rev. Lett. **114**, 158101 (2015).
 - [18] K. Proesmans and C. V. den Broeck, EPL **119**, 20001 (2017).
 - [19] A. Dechant, J. Phys. A-Math. Theor. **52**, 035001 (2018).
 - [20] K. Macieszczak, K. Brandner, and J. P. Garrahan, Phys. Rev. Lett. **121**, 130601 (2018).
 - [21] A. M. Timpanaro, G. Guarnieri, J. Goold, and G. T. Landi, Phys. Rev. Lett. **123**, 090604 (2019).
 - [22] Y. Hasegawa and T. Van Vu, Phys. Rev. Lett. **123**, 110602 (2019).
 - [23] S. Ito and A. Dechant, Phys. Rev. X **10**, 021056 (2020).
 - [24] K. Liu, Z. Gong, and M. Ueda, Phys. Rev. Lett. **125**, 140602 (2020).
 - [25] J. M. Horowitz and T. R. Gingrich, Nat. Phys. **16**, 15 (2020).
 - [26] T. Van Vu and Y. Hasegawa, Phys. Rev. Research **2**, 013060 (2020).
 - [27] T. Koyuk and U. Seifert, Phys. Rev. Lett. **125**, 260604 (2020).
 - [28] Y. Hasegawa, Phys. Rev. Lett. **125**, 050601 (2020).
 - [29] G. Falasco, M. Esposito, and J.-C. Delvenne, New J. Phys. **22**, 053046 (2020).
 - [30] A. Dechant and S. Sasa, Proc. Natl. Acad. Sci. USA **117**, 6430 (2020).
 - [31] J. P. Garrahan, Phys. Rev. E **95**, 032134 (2017).
 - [32] T. R. Gingrich and J. M. Horowitz, Phys. Rev. Lett. **119**, 170601 (2017).
 - [33] G. Falasco and M. Esposito, Phys. Rev. Lett. **125**, 120604 (2020).
 - [34] K. Hiura and S.-i. Sasa, Phys. Rev. E **103**, L050103 (2021).
 - [35] B. Kuznets-Speck and D. T. Limmer, Proc. Natl. Acad. Sci. USA **118**, e2020863118 (2021).
 - [36] A. Pal, S. Reuveni, , and S. Rahav, <https://arxiv.org/abs/2103.16578> (2021).

- [37] N. G. V. Kampen, *Stochastic Processes in Physics and Chemistry* (Elsevier Science & Technology Books, 2007).
- [38] C. W. Gardiner, *Handbook of Stochastic Methods* (Springer, 2010).
- [39] U. Seifert, Phys. Rev. Lett. **95**, 040602 (2005).
- [40] G. Teza and A. L. Stella, Phys. Rev. Lett. **125**, 110601 (2020).
- [41] J. Howard, *Mechanics of Motor Proteins and the Cytoskeleton* (Sinauer Associates and Sunderland, MA, 2001).
- [42] A. B. Kolomeisky, *Motor Proteins and Molecular Motors* (CRC Press, 2015).
- [43] M. L. Mugnai, C. Hyeon, M. Hinczewski, and D. Thirumalai, Rev. Mod. Phys. **92**, 025001 (2020).
- [44] M. J. Schnitzer and S. M. Block, Nature **388**, 386 (1997).
- [45] W. Hua, E. C. Young, M. L. Fleming, and J. Gelles, Nature **388**, 390 (1997).

Supplemental Materials for “entropy production related properties of first passage process”

Yunxin Zhang

Laboratory of Mathematics for Nonlinear Science, Shanghai Key Laboratory for Contemporary Applied Mathematics, Centre for Computational Systems Biology, School of Mathematical Sciences, Fudan University, Shanghai 200433, China.

The probability density $p_k(s, t)$ that a random particle initiated at site k to reach the absorbing boundary N at time t and with EP s satisfies the following backward master equation

$$\partial_t p_k(s, t) = u_k p_{k+1}(s - \ln(u_k/w_{k+1}), t) + w_k p_{k-1}(s - \ln(w_k/u_{k-1}), t) - (u_k + w_k) p_k(s, t), \quad (\text{S1})$$

with $\ln(u_k/w_{k+1})$ and $\ln(w_k/u_{k-1})$ EPs ($k_B = 1$) during one forward and backward jump, respectively [2, 39, 40]. From Eq. (S1), the mean EP $S_k := \int_{-\infty}^{\infty} s \int_0^{\infty} p_k(s, t) dt ds$ during the passage process from site k to boundary N satisfies

$$u_k S_{k+1} + w_k S_{k-1} - (u_k + w_k) S_k = - \left(u_k \ln \frac{u_k}{w_{k+1}} + w_k \ln \frac{w_k}{u_{k-1}} \right). \quad (\text{S2})$$

The mean FPT $T_k := \int_0^{\infty} t \int_{-\infty}^{\infty} p_k(s, t) ds dt$, and the second moment of FPT $T_k^{(2)} := \int_0^{\infty} t^2 \int_{-\infty}^{\infty} p_k(s, t) ds dt$, satisfy

$$u_k T_{k+1} + w_k T_{k-1} - (u_k + w_k) T_k = -1, \quad (\text{S3})$$

$$u_k T_{k+1}^{(2)} + w_k T_{k-1}^{(2)} - (u_k + w_k) T_k^{(2)} = -2T_k. \quad (\text{S4})$$

Meanwhile, the probability density $q_k(n)$ that a random particle initiated at site k to reach the absorbing boundary N with TNJ n satisfies the following backward master equation

$$u_k q_{k+1}(n-1) + w_k q_{k-1}(n-1) - (u_k + w_k) q_k(n) = 0. \quad (\text{S5})$$

From which, the mean TNJ $n_k := \sum_{n=0}^{\infty} n q_k(n)$, and the corresponding second moment $n_k^{(2)} := \sum_{n=0}^{\infty} n^2 q_k(n)$, satisfy

$$u_k n_{k+1} + w_k n_{k-1} - (u_k + w_k) n_k = -(u_k + w_k), \quad (\text{S6})$$

$$u_k n_{k+1}^{(2)} + w_k n_{k-1}^{(2)} - (u_k + w_k) n_k^{(2)} = -(2n_k - 1)(u_k + w_k). \quad (\text{S7})$$

By usual algebraic calculation, one can obtain from Eq. (S2) that

$$S_k = \sum_{l=k}^{N-2} \ln \frac{u_l}{w_{l+1}} = \ln \left(\prod_{l=k}^{N-2} \frac{u_l}{w_{l+1}} \right), \quad (\text{S8})$$

the solution T_k of Eq. (S3) is

$$T_k = \sum_{l=k}^{N-1} \sum_{i=0}^l \left[\frac{1}{u_i} \prod_{j=i+1}^l \left(\frac{w_j}{u_j} \right) \right], \quad (\text{S9})$$

and according to Eq. (S4, S6, S7),

$$T_k^{(2)} = \sum_{l=k}^{N-1} \sum_{i=0}^l \left[\frac{2T_i}{u_i} \prod_{j=i+1}^l \left(\frac{w_j}{u_j} \right) \right], \quad (\text{S10})$$

$$n_k = \sum_{l=k}^{N-1} \sum_{i=0}^l \left[\left(1 + \frac{w_i}{u_i} \right) \prod_{j=i+1}^l \left(\frac{w_j}{u_j} \right) \right], \quad (\text{S11})$$

$$n_k^{(2)} = \sum_{l=k}^{N-1} \sum_{i=0}^l \left[(2n_i - 1) \left(1 + \frac{w_i}{u_i} \right) \prod_{j=i+1}^l \left(\frac{w_j}{u_j} \right) \right]. \quad (\text{S12})$$

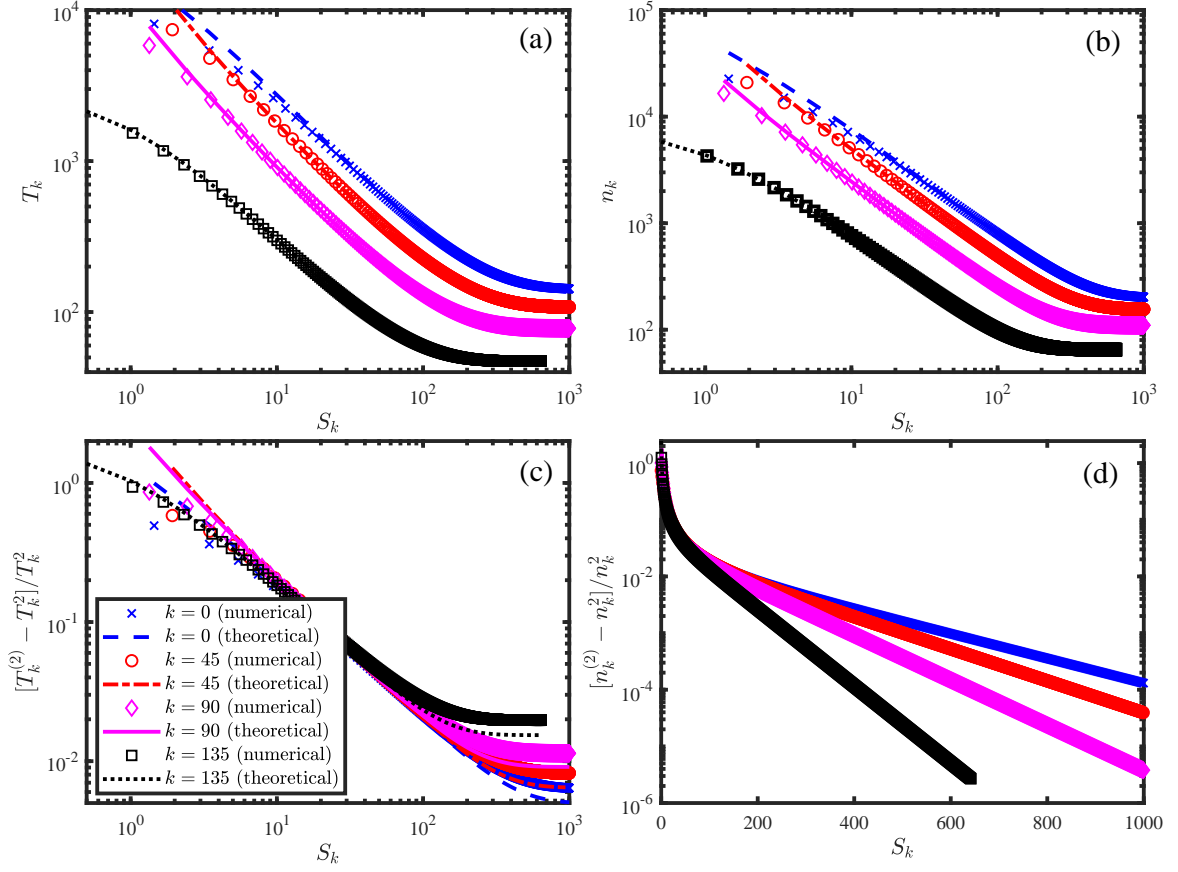


FIG. S1: Similar plots as in Fig. 3. In the first calculation, all forward rates $\{u_k^{(1)}\}$ and backward rates $\{w_k^{(1)}\}$ are randomly selected in interval $(0.5, 3)$. Then in following calculations, forward rates $\{u_k\}$ remain unchanged while backward rates change according to $w_k^{(l+1)} = \gamma w_k^{(l)}$ with $\gamma = 0.99$. Points are obtained numerically by formulations given in Eqs. (S8,S9,S10,S11,S12). The theoretical line for T_k is obtained by $(N - k)/[u(1 - r)]$, and other lines are obtained from the bounds given in Eqs. (15,18,20), respectively. Again, r is replaced by $\exp(-S_k/(N - k - 1))$, and u is replaced by the harmonic mean of $\{u_i\}_{i=k}^{N-1}$.

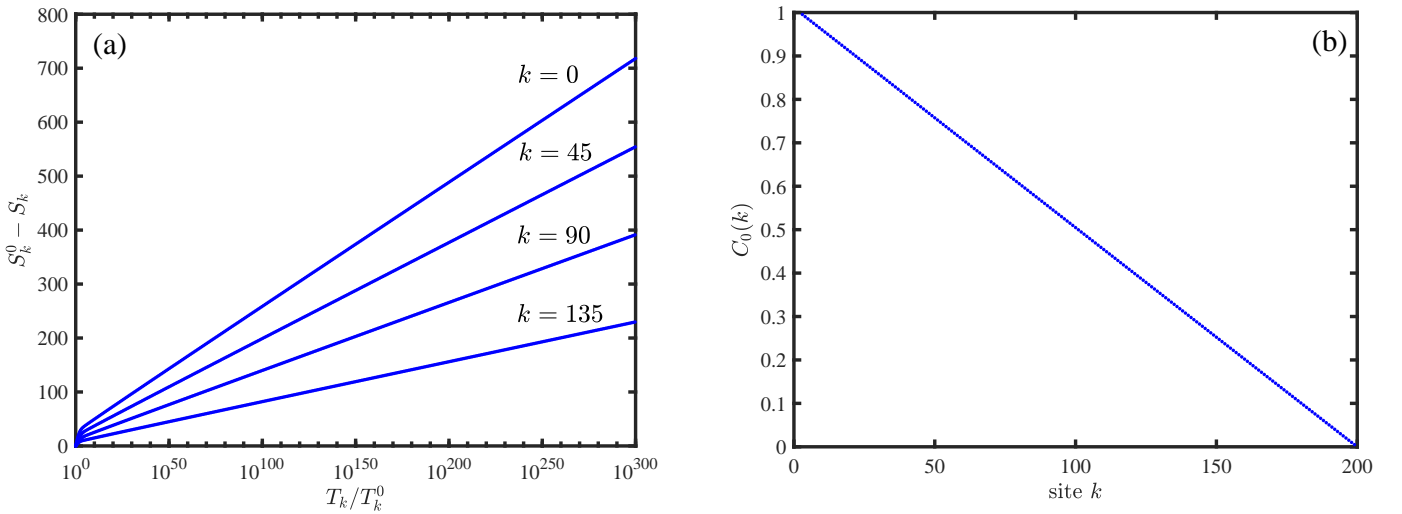


FIG. S2: Similar as in Fig. 2 but with $\gamma = u_k^{(l+1)}/u_k^{(l)} \equiv 0.99$, which means forward rates $\{u_k\}$ tend to zero. (a) $S_k^0 - S_k$ versus T_k/T_k^0 for $k = 0, 45, 90, 135$, and (b) $C_0(k)$ obtained by fitting $T_k/T_k^0 = C_1(k) \exp(-(S_k - S_k^0)/C_0(k))$, see Eq. (21). For $\{u_k\}$ fixed while $\{w_k\}$ increase to infinity, figures (a,b) are almost unchanged, see Eqs. (21,26). Values of S_k and T_k are obtained by Eqs. (S8,S9), respectively.

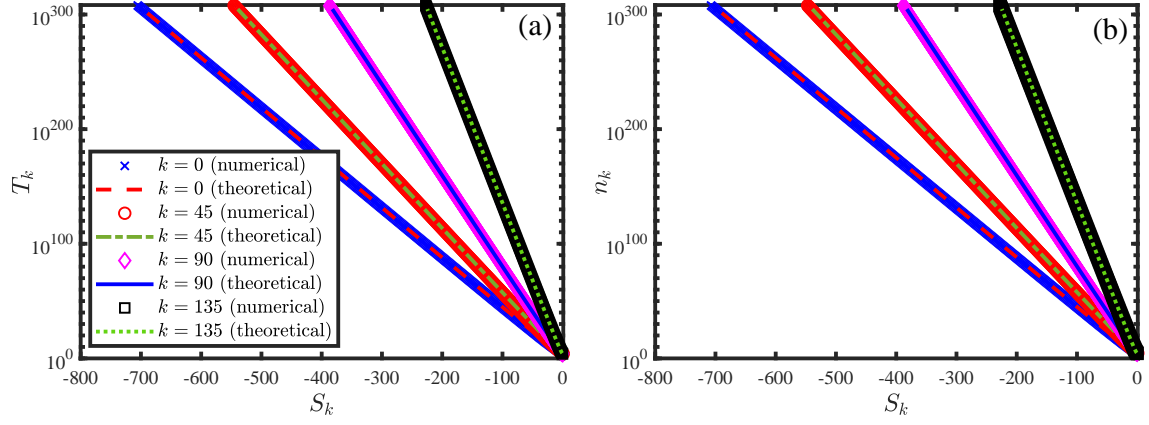


FIG. S3: Similar plots as in Fig. 3, but with parameter values chosen by the same method as in Fig. S2. For these cases, $[T_k^{(2)} - T_k^2]/T_k^2$ and $[n_k^{(2)} - n_k^2]/n_k^2$ are almost constant 1 for $S_k \leq 10$, see Eq. (25).

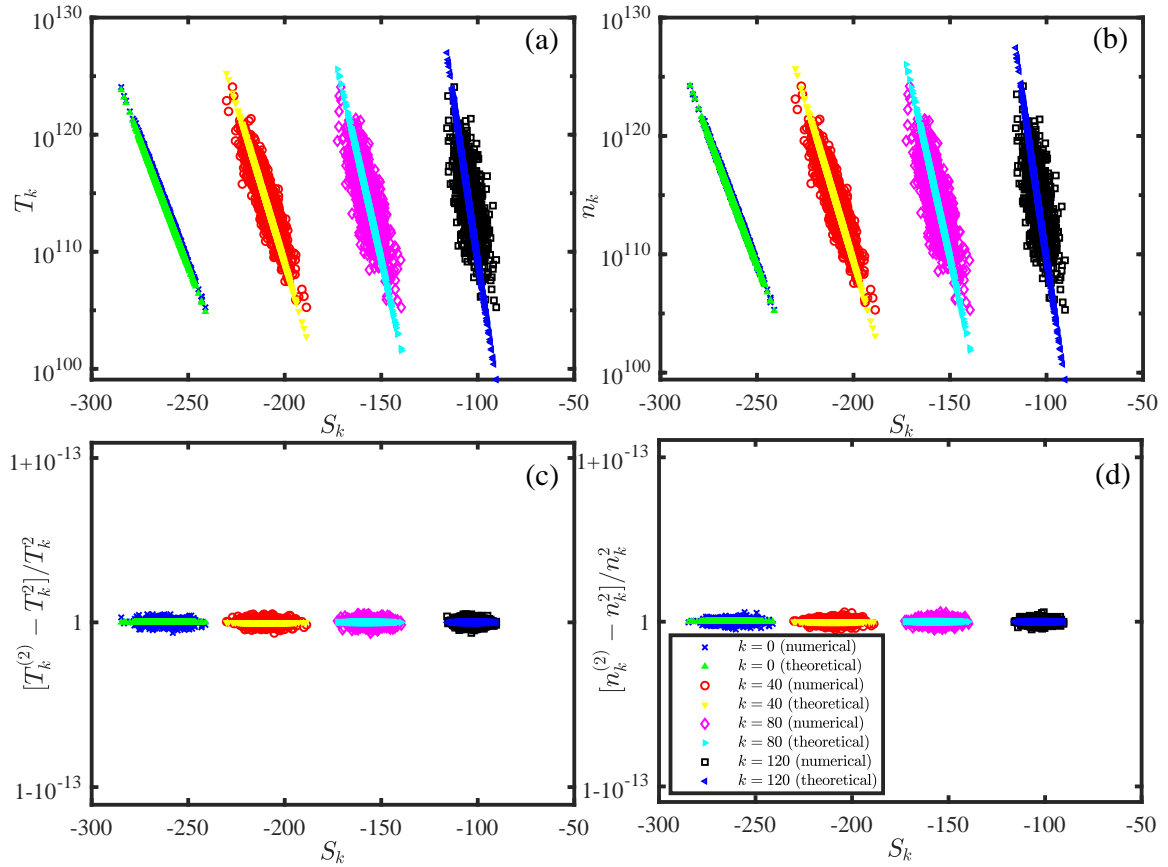


FIG. S4: Similar plots as Fig. 4, but with $\{u_i\}$ are randomly selected in interval $(0.5, 1)$. The theoretical lines (marked by varies triangles) are obtained from the bounds given in Eqs. (22,25), with r replaced by $\exp(-S_k/(N - k - 1))$, and w replaced by the harmonic mean of $\{w_i\}_{i=k}^{N-1}$. Numerical values are obtained by formulations given in Eqs. (S8,S9,S10,S11,S12).

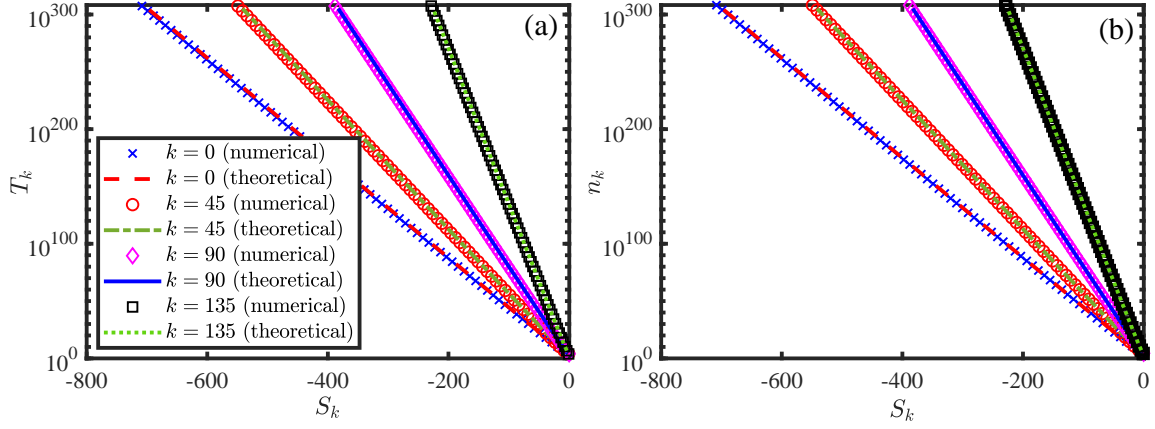


FIG. S5: Similar plots as in Fig. S1, but $w_k^{(l+1)} = \gamma w_k^{(l)}$ with $\gamma = 1.05$.

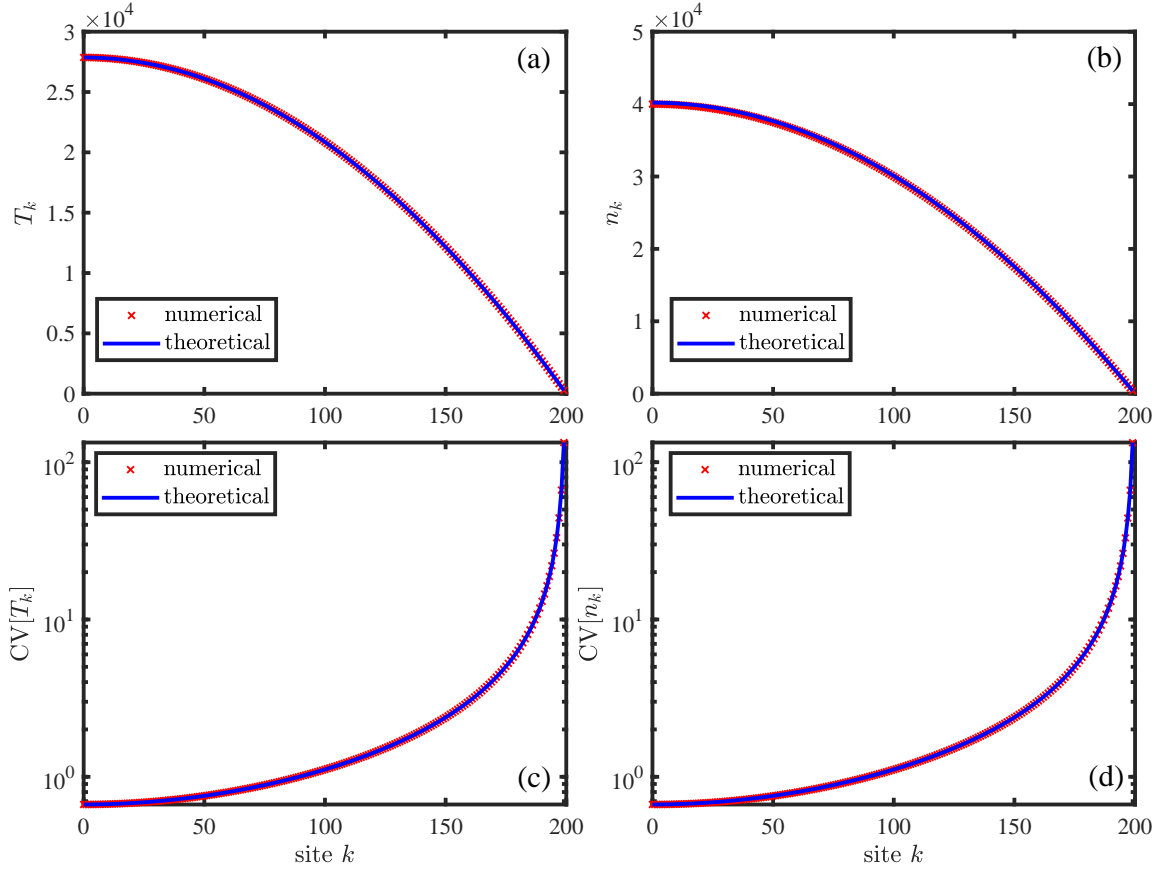


FIG. S6: Mean FPT T_k , mean TNJ n_k and their coefficients of variation $\text{CV}[T_k]$, $\text{CV}[n_k]$ for general equilibrium cases. In each calculations, $\{w_k\}$ are randomly selected in interval $(0.5, 1)$, and then let $u_k = w_k$. The numerical results are obtained by the average of 1000 calculations (see Eqs. (S8,S9,S10,S11,S12) for formulations), and the theoretical ones are obtained according to Eqs. (27,28,29,30), which are derived for the special cases with $u_k \equiv u = w \equiv w_i$ for any k, i .

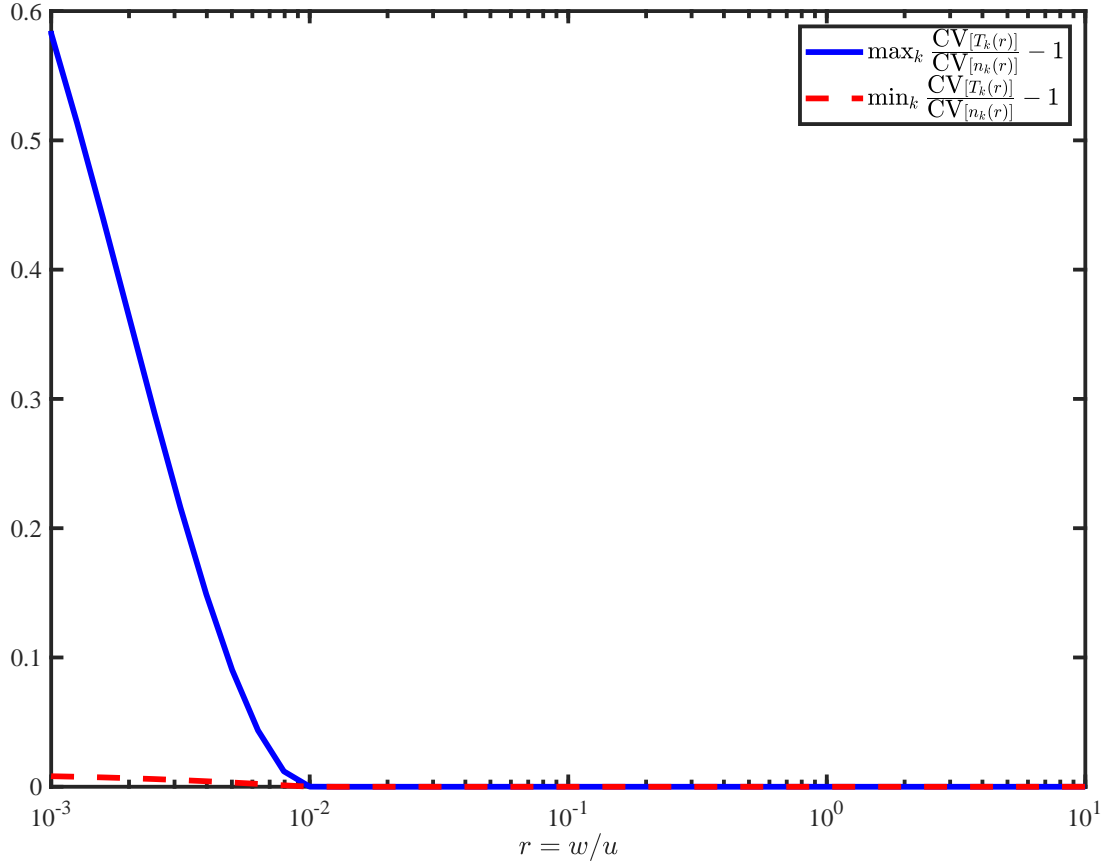


FIG. S7: The maximum and minimum of $\text{CV}[T_k(r)]/\text{CV}[n_k(r)] - 1$, for $N = 100$ and $r = w/u$ changes from 10^{-3} to 10. This plot shows that $\text{CV}[n_k(r)] \leq \text{CV}[T_k(r)]$ holds true for the case with finite states as depicted in Fig. 1(a), and $\text{CV}[n_k(r)] \sim \text{CV}[T_k(r)]$ for large r as obtained in Eq. (25).

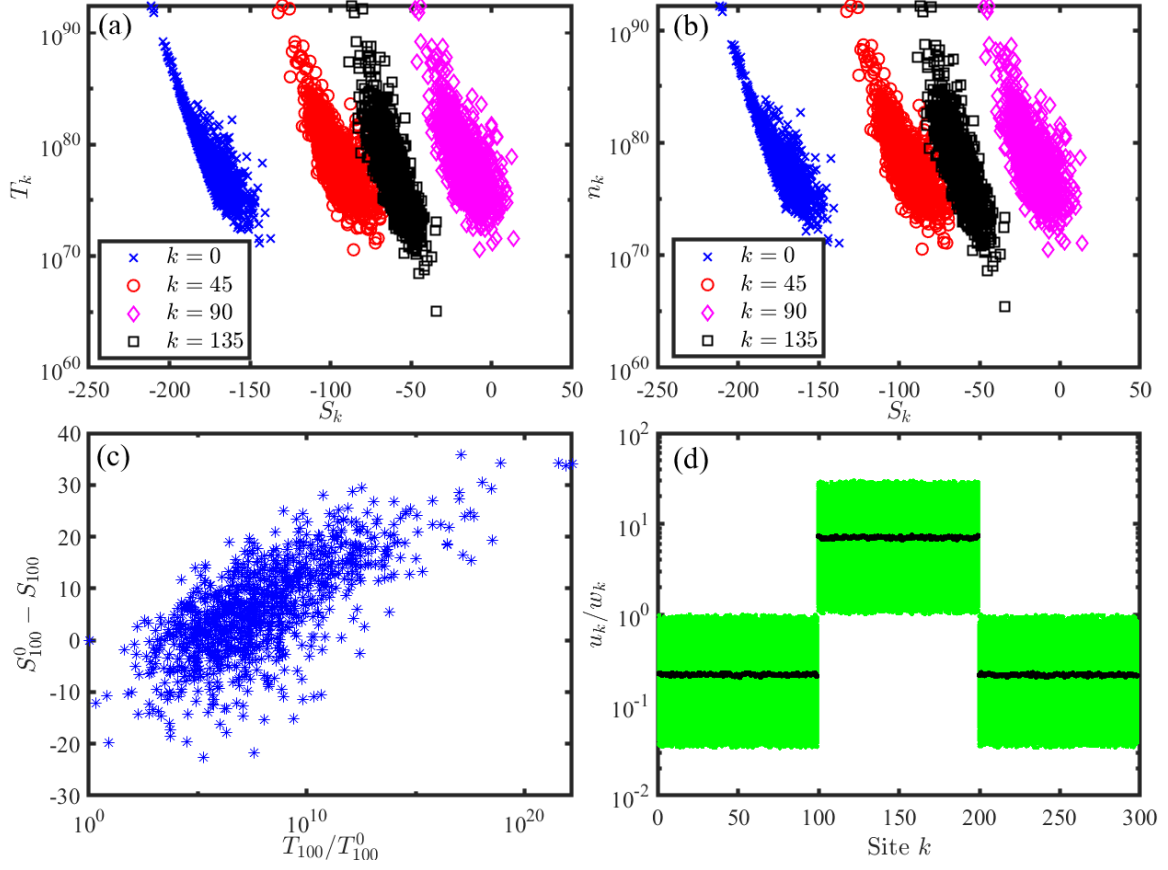


FIG. S8: Results for the first passage process as depicted in Fig. 1(d) (with x_2 assumed to be the absorbing boundary N as in Fig. 1(a)). For $k < 100$ and $k \geq 200$, $\{u_k\}$ and $\{w_k\}$ are randomly selected in intervals $(0.1, 0.5)$ and $(0.5, 3)$ respectively, while for $100 \leq k < 200$ their selection intervals are exchanged with each other. The same as in Fig. 5, $N = 300$ is used, and altogether 1000 groups of $\{u_k\}$ and $\{w_k\}$ are used. In (d), large thick dots represent the mean value of u_k/w_k , and the 1000 values of u_k/w_k are plotted as small light dots.